Journal of Applied Electrochemistry **30**: 187–192, 2000.

Electrosynthesis of hydrogen peroxide by partial reduction of oxygen in alkaline media. Part II: Wall-jet ring disc electrode for electroreduction of dissolved oxygen on graphite and glassy carbon

P. ILEA*, S. DORNEANU and I.C. POPESCU
Department of Physical Chemistry, University "Babes-Bolyai", RO-3400 Cluj-Napoca, Romania
(author for correspondence, e-mail: pilea@chem.ubbcluj.ro)*

Received 19 February 1999; accepted in revised form 27 July 1999

Key words: graphite and glassy carbon electrodes, hydrogen peroxide electrosynthesis, partial oxygen reduction, wall-jet ring disc electrode

Abstract

A wall-jet ring disc electrode was constructed by adapting a wall-jet flow through electrochemical cell. Commercially available spectral graphite and glassy carbon were used as working disc electrodes and the ring electrode was made of stainless steel. The efficiency and rate constants, measured in a planar parallel flow hydrodynamic regime, indicated the partial electroreduction of dissolved oxygen as a quasi-reversible two-electron process for both electrode materials tested.

1. Introduction

The pulp and paper industry remains a promising market for H_2O_2 primarily due to environmental concerns over chlorine based processing [1–4]. Thus, the use of hydrogen peroxide has become an attractive alternative. Among the various ways of producing hydrogen peroxide, the synthesis by partial electroreduction of dissolved oxygen (PERDO) in alkaline media:

$$O_2 + H_2O + 2\,e^- \Leftrightarrow HO_2^- + HO^- \qquad (1)$$
$$E^\circ = -0.065\ V \quad [5]$$

has received attention [6].

However, PERDO has limited applicability due to low oxygen solubility, a low reaction rate [5] and to the following side reaction:

$$O_2 + 2\,H_2O + 4\,e^- \Leftrightarrow 4\,HO^- \qquad (2)$$

One strategy for improving PERDO is the use of modified electrodes with oxygen reduction electrocatalysts, able to increase both the electroreduction selectivity and the reaction rate [6–12].

Carbonaceous materials are often selected as electrode materials because of their intrinsic electrocatalytic properties for PERDO [13] and also because of their advantageous physico-chemical surface properties, when used as substrate for modified electrodes [5, 6]. A preliminary study using cyclic voltammetry without quantitative estimation [14], established that PERDO occurs as an irreversible process at spectral graphite (SG) or glassy carbon (GC) electrodes.

The PERDO efficiency, defined as the average number of electrons transferred (n), is commonly measured by the rotating ring-disc electrode technique [6, 9, 15–19]. However, we preferred the wall-jet ring-disc electrode (WJRDE) since, for a given electrode geometry (disc electrode radius and inlet capillary nozzle diameter), it allows easy operations in various hydrodynamic modes, by simply changing experimental parameters such as the solution flow rate and the distance between the inlet capillary nozzle and the working electrode [20–25]. In the present context, other major advantages of WJRDE [26–28] were taken into consideration: (i) the low consumption of reagents, while the reproducibility remains high; (ii) the constant supply of fresh solution which prevents accumulation of intermediates at the electrode surface; (iii) the nonuniform primary current distribution, particularly useful for mechanistic discrimination.

Based on these considerations we characterized a WJRDE system, constructed from a wall-jet electrochemical cell [29], using $[Fe(CN)_6]^{3-/4-}$ as a standard redox couple. The WJRDE was then used to estimate the kinetic parameters and the efficiency of PERDO at unmodified SG and GC electrodes, operated in a planar parallel flow hydrodynamic regime.

2. Experimental details

2.1. *Reagents and materials*

$K_4[Fe(CN)_6]$, $Na_2SO_4.10\,H_2O$ and NaOH were of analytical grade and were used as received. 0.5 M Na_2SO_4 and 0.1 or 1 M NaOH aqueous solutions were used as supporting electrolytes for WJRDE characterization and for PERDO investigation, respectively. All solutions were prepared with doubly distilled water.

The working disk electrodes were made either of spectral graphite (Ringsdorff-Werke Gmbh, Germany) or of glassy carbon (Tacussel, France). The ring electrode was made of stainless steel (AISI 304).

2.2. *Electrochemical measurements*

The WJRDE system (Figure 1) was a wall-jet electrochemical cell [29] equipped with a homemade ring disc electrode, a Pt wire counter electrode and an Ag/AgCl, KCl 1 M reference electrode. To construct the ring disc electrode, the working disc electrode ($\phi = 3$ mm) and the ring electrode ($\phi_{out} = 6$ mm, $\phi_{inn} = 4$ mm) were mounted in a Perspex body, and were sealed together with epoxy resin. Before use, the ring disc electrode was carefully wet polished with emery paper (grit 400 and 600, Carbochim, Romania) and Al_2O_3 (1 μm). The upper part of the WJRDE, where the ring disc electrode was inserted, has a thread with a 1 mm step, allowing a fine-tuning of the distance (H) between the inlet capillary nozzle ($\phi = 0.5$ mm) and the disc electrode.

The WJRDE was inserted into a single line flow system, consisting of a peristaltic pump (Alitea-XV, Sweden) and silicone tubing (0.16 $cm^3\ m^{-1}$).

The four electrodes of the electrochemical cell were connected to a custom made bipotentiostat, controlled by an IBM-PC (Olivetti 486/33) through a data acquisition card (AT-MIO-16F-5, National Instruments, USA). The software used to monitor the set-up and to perform the data acquisition was written using LabVIEW 3.1.

An oxygen electrode (97-08, Orion Research Inc, USA) measured the dissolved oxygen concentration.

3. Results and discussions

3.1. *WJRDE hydrodynamic characterization*

The limiting current and the collection efficiency (N) observed in a WJRDE are strongly influenced by the hydrodynamic conditions under which the system is operated [23, 23]. On the other hand the potential of the ring electrode has to be in a mass transfer controlled domain.

Consequently, the dependence of the ring current (I_r) on the disc potential was initially recorded at different ring applied potentials, while a 0.01 M $K_4[Fe(CN)_6]$ solution, containing 0.5 M Na_2SO_4 as supporting electrolyte, was pumped through the system ($V_f = 0.29$ $cm^3\ min^{-1}$). To induce progressive oxidation of $[Fe(CN)_6]^{4-}$, the disc electrode potential was linearly swept at a low potential scan rate (10 mV s^{-1}), from +0.05 to +0.6 V vs Ag/AgCl, KCl 1 M. It was noticed (results not shown) that an applied potential value of −0.3 V vs Ag/AgCl, KCl 1 M was sufficiently negative to develop a well-fashioned wave at the ring electrode corresponding to the reduction of $[Fe(CN)_6]^{3-}$, on the disc electrode. Higher negative applied potentials induced a significant increase in background current, probably due to the reduction of oxides on the ring electrode.

The influence of the electrolyte flow rate on the WJRDE response was investigated by maintaining the ring electrode potential (−0.3 V vs Ag/AgCl, KCl 1 M) and the distance between the inlet capillary nozzle and the working electrode constant. As expected [20–23], both the disc current I_d and I_r increased with flow rate (results not shown). However, at flow rates higher than 0.5 $cm^3\ min^{-1}$ the length of the diffusion plateau, for

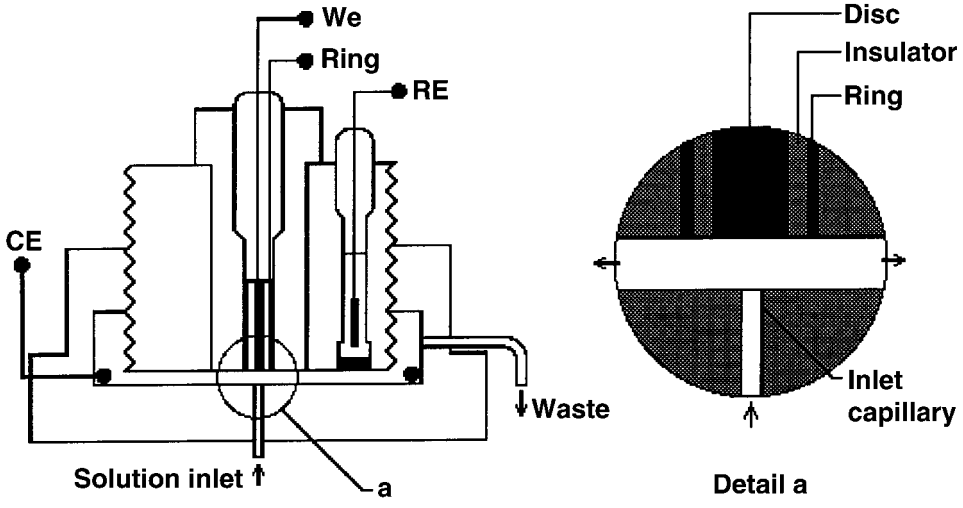

Fig. 1. Scheme of the wall-jet electrochemical cell equipped with a ring-disc electrode.

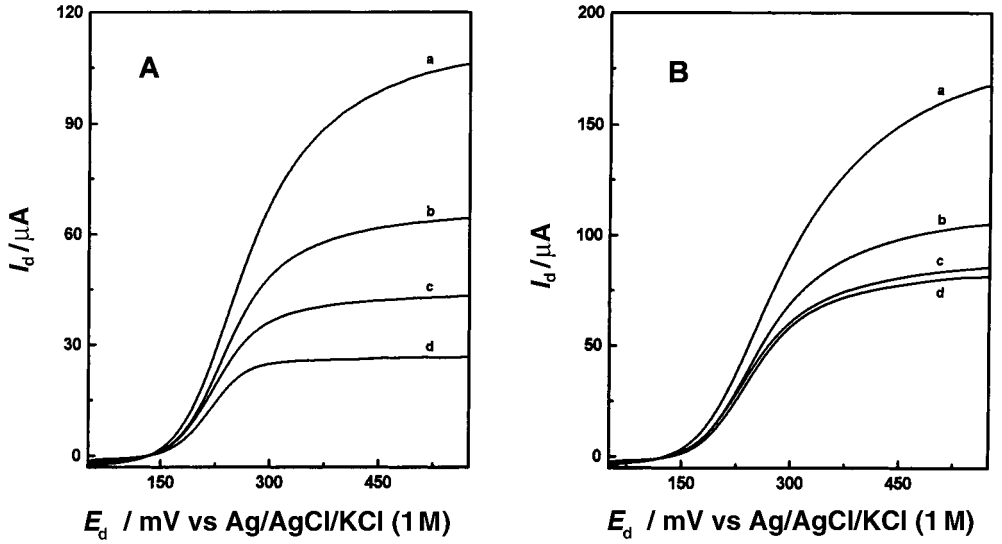

Fig. 2. Polarization curves at WJRDE for a 0.01 M $K_4Fe(CN)_6$ solution, at different distances between the inlet capillary nozzle to electrode: (**a**) 0.25, (**b**) 0.5, (**c**) 1.0 and (**d**) 2.0 mm; and two flow rates: 0.119 cm^3 min^{-1} (**A**); 0.476 cm^3 min^{-1} (**B**). Experimental conditions: disc electrode, spectral graphite; scan rate 2.5 mV s^{-1}; ring electrode potential, −0.3 V vs Ag/AgCl, KCl 1 M.

both disc and ring electrodes, was considerably reduced. Consequently, for all further experiments, the flow rates were limited to values lower than 0.5 cm^3 min^{-1} to increase the precision of the limiting current.

Figure 2 shows the influence of the distance H on the WJRDE response for two different flow rates, with other experimental parameters kept at their previously established values. In accordance with wall-jet electrode theory [20–26, 28], irrespective of the flow rate, the limiting current decreased with increase in H. Once again, taking into account the extension of the diffusion controlled domain, a value of 1 mm was selected for H, for all further measurements. Under these conditions, taking into account the ratio between the inlet capillary nozzle diameter and H, the disc electrode should behave as a wall-jet electrode with a nonuniformly accessible surface [20, 26, 28].

To check this assumption for our experimental set-up we utilized the general Levich equation [24]:

$$i_{l,d} = nFCD^{2/3}KV_f^x \qquad (3)$$

where $i_{l,d}$ is the limiting current density (mA); n is the number of transferred electrons; F is the faradaic constant (A s equiv^{-1}); C is concentration of the electrochemical active species (mM L^{-1}); D is diffusion coefficient (m^2 s^{-1}); K is a constant depending on electrolyte viscosity and the geometry of the electrochemical cell and V_f is the solution flow rate (cm^3 s^{-1}). The flow rate exponent (x) was estimated at different H values, as the slope of the linear correlation between $\log(i_{l,d}/\mu A\ cm^{-2})$ and $\log(V_f/cm^3\ min^{-1})$.

The values obtained and the corresponding hydrodynamic regimes are presented in Table 1.

Finally, a planar parallel flow (PPF) hydrodynamic regime ($H = 1$ mm in Table 1) was selected for conducting the PERDO study because it presented the smallest difference between the expected and obtained x values.

For the PPF hydrodynamic regime the average collection efficiency (N) values, measured for both the SG and GC disc electrodes, were 0.34 ± 0.02 and 0.21 ± 0.03, respectively, for flow rates between 0.1 to 0.5 cm^3 min^{-1}. The variation of the collection efficiency with the nature of the disc material is possibly due to the inherent shortcomings in fabrication which may be different from electrode to electrode.

3.2. *PERDO at spectral graphite and glassy carbon WJRDEs*

Linear sweep voltammograms at WJRDE incorporating SG and GC disc electrodes were recorded for the PPF

Table 1. Dependence of the hydrodynamic regime on the distance between the inlet capillary nozzle and disc electrode
For experimental conditions see Figure 2

d/mm	Flow rate exponent, x	Corr. coeff. /no. of points	Hydrodynamic regime [24]
0.25 0.5	0.29 ± 0.02* 0.36 ± 0.01*	0.995/4 0.999/4	$i_{l,d} = 1.47\ nFCD^{2/3}\ (A/b)^{2/3} \times V_f^{1/3}$ thin layer (TL)
1	0.51 ± 0.02*	0.999/4	$i_{l,d} = 0.68\ nFCD^{2/3}\ v^{-1/6} \times (A/b)^{1/2}\ V_f^{1/2}$ planar parallel flow (PPF)
2	0.80 ± 0.03*	0.998/4	$i_{l,d} = 0.898\ nFCD^{2/3}\ v^{-5/12} \times a^{-1/2}\ A^{3/8}\ V_f^{3/4}$ wall-jet (WJ)

* Standard deviation

a = inlet cappilary nozzle diameter; A, electrode area; b = channel height; C = concentration (mM L^{-1}); F = Faraday constant; D = diffusion coefficient; v = kinematic viscosity; V_f = volume flow rate; n = number of electrons.

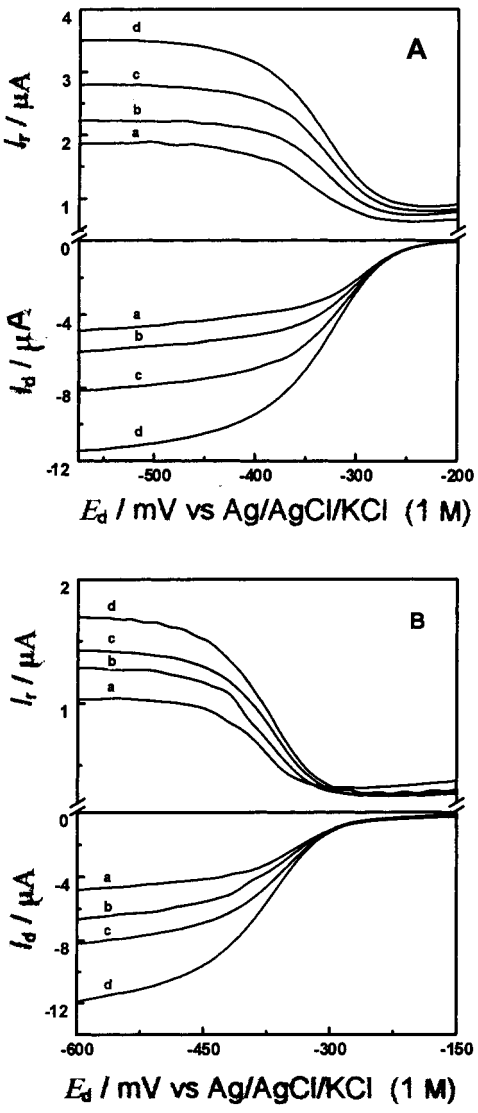

Fig. 3. WJRDE polarization curves for reduction of the dissolved O_2, at different flow rates: (**a**) 0.119, (**b**) 0.238; (**c**) 0.476 and (**d**) 0.952 cm^3 min^{-1}; (**A**) spectral graphite disc electrode; (**B**) glassy carbon disc electrode. Experimental conditions: scan rate 2.5 mV s^{-1}; supporting electrolyte, 1 M NaOH; ring electrode potential, +0.5 V vs Ag/AgCl/KCl 1 M; $H = 1$ mm.

hydrodynamic regime at different flow rates. As pointed out by Compton et al. [28], in order to obtain a steady-state voltammetric response it is decisivly important to use, for a given flow rate, a sufficiently low potential scan rate. In our case, a scan rate of 2.5 mV s^{-1} was found to assure a real stationary voltammogram, proved by the absence of hysteresis when the scan direction was reversed in the investigated potential range. The WJRDE responses showing the dissolved oxygen reduction at disc electrode and the resulting H_2O_2 oxidation at ring electrode are presented in Figure 3, for both investigated electrode materials.

Table 2. PERDO current efficiency at disk electrodes made of different electrode materials
For experimental conditions see Figure 3

V_f/cm^3 min^{-1}	Current efficiency/%	
	Spectral graphite	Glassy carbon
0.119	74.6	70.1
0.238	75.2	79.5
0.476	81.1	91.6

The concentration of the dissolved oxygen in the supporting electrolyte (1 M NaOH aqueous solution) was 9 ppm, corresponding to the equilibrium value in experimental conditions. In a preliminary study it was found that an applied potential of +0.5 V vs Ag/AgCl, KCl 1 M corresponds to an efficient H_2O_2 oxidation at ring electrode, associated with a negligible background current.

To estimate the PERDO current efficiency, the charge quantities involved in the dissolved oxygen reduction at disc electrode (q_{O_2}) and in the H_2O_2 oxidation at ring electrode ($q_{H_2O_2}$) were measured by integrating the curves from Figures 3A and 3B (after background current correction). Within the experimental margin of error, the PERDO current efficiency, expressed as the $q_{H_2O_2}/(Nq_{O_2})$ (%) ratio (Table 2), revealed that, irrespective of the electrode material, the reduction of dissolved oxygen occurred predominantly with H_2O_2 production. The current efficiency slightly increased with the flow rate.

Another way to estimate the PERDO efficiency is based on the evaluation of the average number (n) of the transferred electrons involved in the cathodic reduction of the dissolved oxygen. For this purpose we used the equation proposed by Claude et al. [30]:

$$n = \frac{4i_{l,d}}{(i_{l,d} + i_{l,r}/N)} \tag{4}$$

Table 3. Experimental values of the flow rate exponent (x) for disc (glassy carbon and spectral graphite) and ring (stainless steel) electrodes corresponding to $Fe[(CN)_6]^{4-}$ oxidation and dissolved oxygen reduction
Experimental conditions: flow rate range, 0.1 to 0.5 cm^3 min^{-1}; for other conditions see Figure 3

Electrochemical active species	Flow rate exponent, x			
	Spectral graphite		Glassy carbon	
	Disc	Ring	Disc	Ring
$[Fe(CN)_6]^{4-}$	0.51 ± 0.02*	0.40 ± 0.01*	0.54 ± 0.03*	0.32 ± 0.02*
O_2 in NaOH 0.1 M	0.50 ± 0.01*	0.39 ± 0.03*	0.53 ± 0.01*	0.33 ± 0.01*
O_2 in NaOH 1 M	0.51 ± 0.03*	0.40 ± 0.01*	0.53 ± 0.04*	0.32 ± 0.03*

* Standard deviation

where $i_{l,d}$, $i_{l,r}$ stand for limiting current densities for disc and ring electrode, respectively, and N is the collecting efficiency. Checking the validity of the PPF hydrodynamic regime proved the invariance of the measured collecting efficiency, when $[Fe(CN)_6]^{4-}$ was replaced by NaOH. Within the experimental error, it was found that the hydrodynamic regime remains unchanged ($x \sim 0.5$), for a flow rate range of 0.1 to 0.5 $cm^3\ min^{-1}$ (Table 3).

Table 4 displays the average number (n) of electrons transferred during the cathodic reduction of the dissolved oxygen into two supporting electrolyte concentrations. The computed n values confirm the previous conclusion that the two-electron reduction of dissolved oxygen is the only cathodic process occurring at disc electrodes made of SG or GC.

Taking into account that for both electrode materials the dissolved oxygen is electroreduced only to H_2O_2, an approach based on the Levich treatment of the WRJDE response was used to estimate the rate constant for PERDO. The reciprocal value of the disc current ($1/I_d$) was plotted against the reciprocal value of the flow rate square root ($V_f^{-1/2}$) (Figures 4(A) and 4(B)), at different constant values of the disc applied potential. The applied potential values were selected from the mixed control (activation/diffusion) domain. The pure charge transfer current densities (i_{ct}) were computed by linear extrapolation at infinite flow rate of the above-mentioned correlation. Subsequently, the electrochemical rate constants (k_f) for the heterogeneous electron transfer were estimated using the equation:

$$i_{ct} = nk_fFC_{O_2} \tag{5}$$

where $k_f = k^\circ \exp(-\alpha n\eta/RT)$, C_{O_2} stands for dissolved oxygen concentration, $\eta = E - E^{\circ'}$ and $E^{\circ'}$ is the formal standard potential for the Reaction 1. Finally, a Tafel plot allowed for the evaluation of the standard rate constant (k°).

Table 4. Average number of electrons transferred in the electroreduction of dissolved oxygen at graphite and glassy carbon disc electrodes For experimental conditions see Table 3

[NaOH]/M	Average number of electrons transferred	
	Glassy carbon	Spectral graphite
1	2.17 ± 0.03*	2.00 ± 0.01*
0.1	1.92 ± 0.10*	2.10 ± 0.05*

* Standard deviation

It is worth noting that the k° values (Table 5) are higher for SG than for GC electrodes, pointing out that SG has a higher intrinsic electrocatalytic activity for oxygen electroreduction. This behaviour occurs very likely due to the presence of oxygen-containing groups on the SG surface. This supposition is supported by Paliteiro et al. [13] reporting an even higher k° value for electrodes of oxidized pyrolytic graphite.

Finally, it should be mentioned that in spite of the fact that the wall-jet electrode surface is not uniformly accessible in terms of mass transport [27], it has been already used for kinetic investigations according to the approach described above [31–33]. Moreover, a comparison between the results obtained, for the kinetics of direct and mediated electroreduction of hydrogen peroxide at peroxidase modified graphite electrodes, with WJRDE and rotating disc electrode revealed no significant difference [33]. This concordance should be expected if the charge transfer is quite irreversible and can be evidenced by a good linearity of the Levich reciprocal plot.

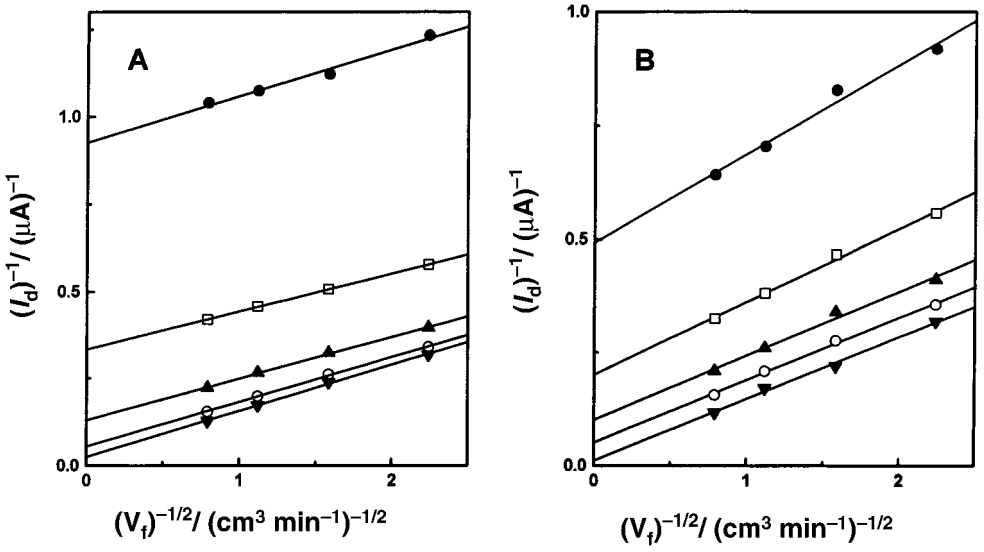

Fig. 4. Dependence of the reciprocal current intensity at disc electrode (I_d^{-1}) on the reciprocal square root value of the flow rate ($V_f^{-1/2}$), for reduction of dissolved O_2 at different constant values of the disc applied potential. (**A**) Spectral graphite electrode: (●) 0.275, (□) 0.300, (▲) 0.325; (○) 0.350 and (▼) 0.375 V vs Ag/AgCl/KCl 1 M; (**B**) Glassy carbon electrode: (●) 0.325, (□) 0.350, (▲) 0.375; (○) 0.400 and (▼) 0.450 V vs Ag/AgCl/KCl 1 M. For experimental conditions see Figure 3.

Table 5. Heterogeneous rate apparent constants for electroreduction of the dissolved oxygen
For experimental conditions see Table 3

Electrode material	NaOH/M	log $k°$/cm s^{-1}	Corr. coeff.* /no. of points
Spectral graphite	1	$-3.27 \pm 0.02^{\dagger}$	0.999/4
	0.1	$-4.43 \pm 0.10^{\dagger}$	0.999/4
Glassy carbon	1	$-3.67 \pm 0.04^{\dagger}$	0.999/5
	0.1	$-4.78 \pm 0.08^{\dagger}$	0.998/5

* Tafel correlation
† Standard deviation

4. Conclusions

Using a wall-jet ring-disc electrode, operating in a planar parallel flow regime, the partial electroreduction of dissolved oxygen occurs as a quasi-reversible two-electron process both on spectral graphite and glassy carbon electrodes: $k° \sim (1.3 \pm 0.1) \times 10^{-5}$ m s^{-1} and $(0.7 \pm 0.1) \times 10^{-5}$ m s^{-1}, respectively.

Acknowledgements

Financial support from CNCSU (grant 214/100) is gratefully acknowledged. The single line flow system was a kind gift from Dr Lo Gorton, Lund University, Sweden. The authors thank Adrian Nicoara for the data acquisition software. I.C.P. acknowledges for a Swedish Institute scholarship.

References

1. E.E. Kalu and C. Oloman, *J. Appl. Electrochem.* **20** (1990) 932.
2. B.V. Tilak, *in* J.D. Genders and N.L. Weinberg (Eds), 'Electrochemistry for a Cleaner Environment', (The Electrosynthesis Company, New York, 1992), p. 387.
3. J.A. McIntyre, *The Electrochemical Society Interface*, **4**, Spring (1995) 29.
4. O. Savadogo and S. Leclerc, Résumés des Comunications, Journées d'Electrochimie, Montréal (1997), Abstract COP-4.
5. K. Kinoshita, 'Electrochemical Oxygen Technology' (J. Wiley & Sons, New York, 1992), p.32.
6. A. Elzing, A. Van der Putten, W. Visscher and E. Barendrecht, *J. Electroanal. Chem.* **233** (1987) 99.
7. A. Elzing, A. van der Putten, W. Visscher and E. Barendrecht, *J. Electroanal. Chem.* **233** (1987) 113.
8. T. Hyodo, M. Hayashi, N. Miura and N. Yamazoe, *J. Electrochem. Soc.* **143** (1996) L266.
9. B. Schubert, E. Gocke, R. Schöllhorn, N. Alonso-Vante and H. Tributsch, *Electrochim. Acta* **41** (1996) 1471.
10. N. Heller-Ling, M. Prestat, J.-L. Gautier, J.-F. Koenig, G. Poillerat and P. Chartier, *Electrochim. Acta* **42** (1997) 197.
11. M. Sadakane and E. Steckhan, *Chem. Rev.* **98** (1998) 219.
12. P. Tatapudi and J.M. Fenton, *J. Electrochem. Soc.* **140** (1993) L55.
13. C. Paliteiro, A. Hamnett and J.B. Goodenough, *J. Electroanal. Chem.* **233** (1987) 147.
14. P. Ilea, S. Dorneanu and A. Nicoara, *Rev. Roumaine Chim.* (1998), in press.
15. Yu. V. Pleskov and V. Yu. Filinovskii, 'The Rotating Disc Electrode' (Consultant Bureau, New York, 1976).
16. R. Greef, R. Peat, L.M. Peter, D. Pletcher and J. Robinson, 'Instrumental Methods in Electrochemistry' (Ellis Horwood, Chichester, 1985), p. 139.
17. C.M.A. Brett and A.M. Oliveira Brett, 'Electrochemistry: Principles, Methods, and Applications' (Oxford University Press, Oxford, 1993), p. 167.
18. S. Strbac, N.A. Anastasijevic and R.R. Adzic, *Electrochim. Acta* **39** (1994) 983.
19. P.T. Kissinger and W.R. Heineman, 'Laboratory Techniques in Electroanalytical Chemistry' (Marcel Dekker, New York, 1996) p. 116.
20. Y. Yamada and H. Matsuda, *J. Electroanal. Chem.* **44** (1973) 189.
21. F. Coeuret, *Chem. Eng. Sci.* **30** (1975) 1257.
22. W.J. Albery and C.M.A. Brett, *J. Electroanal. Chem.* **148** (1983) 201.
23. W.J. Albery and C.M.A. Brett, *J. Electroanal. Chem.* **148** (1983) 211.
24. H. Gunasingham and B. Fleet, *in* A.J. Bard (Ed.), 'Electroanalytical Chemistry', Vol. 16 (Marcel Dekker, New York, 1989), p. 96.
25. B. Soucaze-Guillous and W. Kutner, *Electroanalysis* **9** (1997) 32.
26. D.-T. Chin and C-H. Tsang, *J. Electrochem. Soc.* **125** (1978) 1461.
27. R.G. Compton, C.R. Greaves and A.M. Waller, *J. Appl. Electrochem.* **20** (1990) 575.
28. R.G. Compton, A.C. Fisher and M.A. Latham, *J. Phys. Chem.* **96** (1992) 8363.
29. R. Appelqvist, G. Marko-Varga, L. Gorton, A. Torstensson and G. Johansson, *Anal. Chim. Acta* **169** (1985) 237.
30. E. Claude, T. Addou, J.M. Latour and P. Aldebert, *J. Appl. Electrochem.* **28** (1998) 57.
31. T. Ruzgas, L. Gorton, J. Emneus and G. Marko-Varga, *J. Electroanal. Chem.* **391** (1995) 41.
32. A.A. Karyakin, E.E. Karyakina and L. Gorton, *J. Electroanal. Chem.* **456** (1998) 97.
33. A. Lindgren, F.-D. Munteanu, I. Gazaryan, T. Ruzgas and L. Gorton, *J. Electroanal. Chem.* **458** (1998) 113.